Subarray Beam-Space Adaptive Beamforming for a Dynamic Long Towed Array

Yung P. Lee and Herbert Freese
SAIC
phone: 703-676-6512
email: yung.p.lee@saic.com
email: herbert.a.freese@saic.com

William W. Lee
University of Maryland
email: willee@wam.umd.edu

Abstract In the fast time-varying shallow water environment, the phone-space adaptive processing using sample-matrix-inversion (SMI) approach outperforms the iterative least-mean-squared (LMS) approach due to its rapid convergence. The SMI approach uses singular-value-decomposition (SVD) to decompose a sample-matrix into a set of spatial eigenvectors and their associated eigenvalues. Adaptive beamforming is applied by matching the steering vectors with the spatial eigenvectors weighted by their eigenvalues. When a long towed-array undergoes significant maneuvering, the array shape and/or the target-to-array relative geometry changes rapidly within a processing interval. A signal in the phone-space sample-matrix is split into more than one eigenvector resulting in signal mismatch in the subsequent beamforming. Its power is split into many eigenvalues resulting in signal loss in the processing.

In subarray beam-space adaptive beamforming (SABS ABF), a beam-space sample-matrix is formed at each search cell by focusing subarrays to a cell using the dynamically updated array shape at each time step. The SMI adaptive beamforming then is done by decomposing the beam-space sample-matrix and matching the beam-eigenvectors with a unity steering vector. The beam-space sample-matrix has a lower rank than the phone-space sample-matrix so that a stable estimation can be reached with fewer time samples. The dynamic array shape compensation in SABS ABF makes a signal in the beam-space sample-matrix less likely to be split by the SVD. The subsequent processing, after the SVD, experiences less signal mismatch and signal loss. A dynamic cable model is used to simulate a long towed-array going through turns in a measured shallow water current field. Simulations show that significant signal loss in phone-space SMI processing is recovered in SABS ABF processing.

Report Documentation Page

Form Approved
OMB No. 0704-0188

1. REPORT DATE **20 DEC 2004**	2. REPORT TYPE **N/A**	3. DATES COVERED **-**

4. TITLE AND SUBTITLE **Subarray Beam-Space Adaptive Beamforming for A Dynamic Long Towed-Array**	5a. CONTRACT NUMBER 5b. GRANT NUMBER 5c. PROGRAM ELEMENT NUMBER
6. AUTHOR(S)	5d. PROJECT NUMBER 5e. TASK NUMBER 5f. WORK UNIT NUMBER
7. PERFORMING ORGANIZATION NAME(S) AND ADDRESS(ES) **Science Applications International; University of Maryland**	8. PERFORMING ORGANIZATION REPORT NUMBER
9. SPONSORING/MONITORING AGENCY NAME(S) AND ADDRESS(ES)	10. SPONSOR/MONITOR'S ACRONYM(S) 11. SPONSOR/MONITOR'S REPORT NUMBER(S)

12. DISTRIBUTION/AVAILABILITY STATEMENT
Approved for public release, distribution unlimited

13. SUPPLEMENTARY NOTES
See also, ADM001741 Proceedings of the Twelfth Annual Adaptive Sensor Array Processing Workshop, 16-18 March 2004 (ASAP-12, Volume 1)., The original document contains color images.

14. ABSTRACT

15. SUBJECT TERMS

16. SECURITY CLASSIFICATION OF:			17. LIMITATION OF ABSTRACT	18. NUMBER OF PAGES	19a. NAME OF RESPONSIBLE PERSON
a. REPORT	b. ABSTRACT	c. THIS PAGE			
unclassified	**unclassified**	**unclassified**	**UU**	**27**	

Standard Form 298 (Rev. 8-98)
Prescribed by ANSI Std Z39-18

Subarray Beam-Space Adaptive Beamforming for A Dynamic Long Towed-Array

Yung P. Lee, Herbert Freese
Science Applications International Corporation

William W. Lee
University of Maryland

Abstract:

In the fast time-varying shallow water environment, the phone-space adaptive processing using sample-matrix-inversion (SMI) approach outperforms iterative least-mean-squared (LMS) approach due to its rapid convergence. The SMI approach uses singular-value-decomposition (SVD) to decompose a block sample-matrix into a set of spatial singular vectors and their associated singular values. Adaptive beamforming is applied by matching the steering vectors with the spatial singular vectors weighted by their singular values. When a long towed-array undergoes significant maneuvering, its shape relative to a target changes rapidly within a processing interval. The target signal in the phone-space sample-matrix is split into more than one singular vector resulting signal mismatch in the subsequent beamforming. Its power is split into many singular values resulting signal loss in the processing.

In subarray beam-space adaptive beamforming (SABS_ABF), a beam-space sample-matrix is formed at each search cell by focusing subarrays to a cell using the dynamically updated array shape at each time step. The SMI adaptive beamforming then is done by decomposing the beam-space sample-matrix and matching the beam-eigenvectors with a unity steering vector. The beam-space sample-matrix has a lower rank than the phone-space sample-matrix so that a stable estimation can be reached with fewer time samples. The dynamic array shape compensation in SABS_ABF makes a signal in the beam-space sample-matrix less likely to be split by the SVD. The subsequent processing, after the SVD, experiences less signal mismatch and signal loss. A hydrodynamic cable model is used to simulate a long towed-array going through turns in a measured shallow water current field. Simulations show that significant signal loss in the phone-space adaptive processing is recovered in the SABS_ABF processing.

1. Introduction

There are three main issues for a long towed-array going through dynamic maneuvering, they are increasing of array self-noise, rapid changing in array shape (array element location AEL), and signal spreading in the phone-space sample-matrix. Premus et. al. [1] showed the use of a beam-space adaptive beamforming for towed array self-noise cancellation. Ianniello et. al. [2] demonstrated array shape estimation through turns using a hydrodynamic model with data from the non-acoustic heading and depth sensors. This paper addresses the issue of signal spreading that the received signal on an array changes within the processing interval due to array motion.

Figure 1 shows the simulation scenario using in this

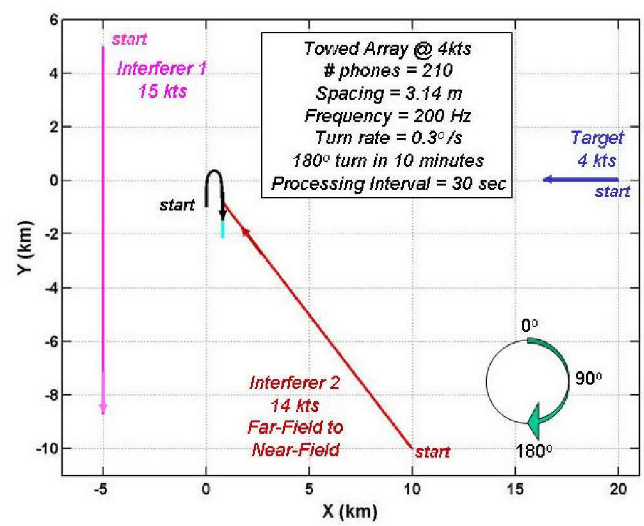

Figure 1: Simulation Geometry

study. A towed ship heads toward North at the beginning of the simulation, it makes an 180° turn in 10 minutes then heads toward South. A long array with 210 hydrophones and a spacing of 3.14 m is towed behind the ship with the first phone at 360 m from the ship. A hydrodynamic cable model is used to simulate a realistic motion of the array going through the turn in a measured shallow water current field. A target starts at a distance of 20 km and approaches the ship from East at a speed of 4 kts. In additional to the own-ship, two other interferers are included to simulate a stressful environment. One interferer starts from North-West, it crosses the back-beam of the target and heads to South. The other starts from South-East and moves into the near-field of the array. The simulation is done at 200 Hz with a sampling rate of every half second. All processing in this study uses a time interval of 30 seconds. True bearing is used for displaying the beamforming results.

Let $x_n(t)$ be the received time series of the n^{th} hydrophone, the signal coherence (SC) relative to the first hydrophone is defined as

$$SC_n(t) = \frac{\left|\sum_{k=0}^{K-1} x_1^*(t + k\Delta t) \bullet x_n(t + k\Delta t)\right|^2}{\sum_{k=0}^{K-1}\left|x_1(t + k\Delta t)\right|^2 \bullet \sum_{k=0}^{K-1}\left|x_n(t + k\Delta t)\right|^2}$$

here K=60 and Δt=0.5 s. For target only, Figure 2 shows

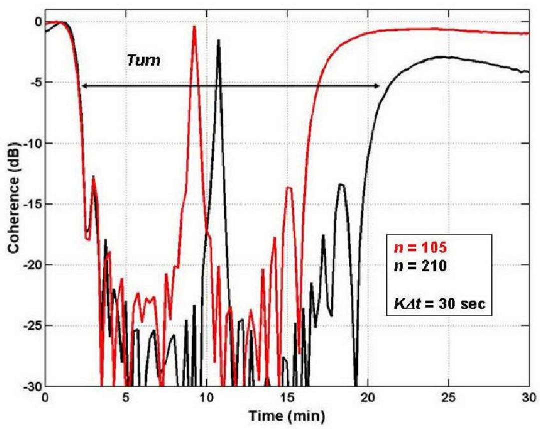

Figure 2: Time histories of signal coherence relative to phone one

the time history of signal coherence for hydrophone in the middle of the array (n=105) and at the end of the array (n=210),respectively. The signal coherence is close to perfect across array before the turn and is significantly degraded in the turn. The effect of the residual tail motion after the turn is seen in hydrophone 210.

Let X be a phone-space sample-matrix for a processing interval $K\Delta t$ and

$$= \begin{bmatrix} x_1(t) & x_1(t+\Delta t) & x_1(t+2\Delta t) & \dots & x_1(t+(K-1)\Delta t) \\ x_2(t) & x_2(t+\Delta t) & x_2(t+2\Delta t) & \dots & x_2(t+(K-1)\Delta t) \\ \vdots & \vdots & \vdots & \vdots & \vdots \\ x_N(t) & x_N(t+\Delta t) & x_N(t+2\Delta t) & \dots & x_N(t+(K-1)\Delta t) \end{bmatrix}$$

After singular-value-decomposition (SVD), X can be written as

$$X = V^{+}\boldsymbol{\Lambda}U$$

where V and U are orthogonal matrices, and Λ is a diagonal matrix

$$\boldsymbol{\Lambda} = \begin{bmatrix} \sqrt{\lambda_1} & 0 & \cdots & 0 \\ 0 & \sqrt{\lambda_2} & \cdots & 0 \\ \vdots & \vdots & \ddots & \vdots \\ 0 & 0 & \cdots & \sqrt{\lambda_N} \end{bmatrix}$$

The columns v_i and u_i of V and U are called the left and right singular vectors, respectively, and the diagonal elements λ_i of Λ are called the singular values. Physically, each v_i represents a spatial structure of a signal observed across the array of hydrophones, the associated u_i contains the information of temporal variation of this signal, and λ_i is the mean power of the observed signal. For target only, Figure 3 shows the singular-value time

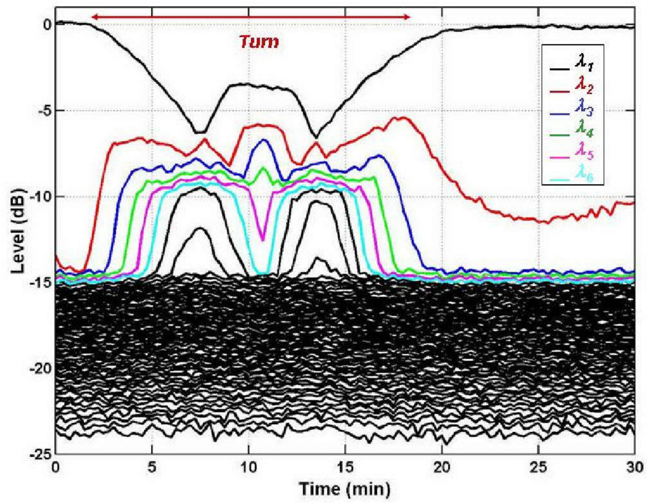

Figure 3: Singular-Value time histories of the phone-space sample-matrix for target only

histories. It shows that target energy is contained within one singular value before the turn and is spread into several singular values in the turn. Without an appropriate signal model to account for the spread, target estimation using the phone-space sample-matrix will be significantly degraded.

Subarray beam-space processing is a two-stage processing. In the first stage, a phone-space sample-matrix is transformed into a beam-space sample-matrix using the dynamically updated AEL. The transformation compensates the temporal variation of the received signal on the array due to rapid changes in array shape. The signal in the beam-space sample-matrix is more stationary and experiences less spread so that the subsequent processing can achieve the optimal result. This paper is organized as follows: Section 2 reviews the white-noise-constrained adaptive beamforming, Section 3 describes the subarray beam-space adaptive beamforming (SABS_ABF), Section 4 shows the simulation results, and Section 5 summaries the study.

2. White-Noise-Constrained (WNC) Adaptive Beamforming

Adaptive processing uses the measured signal plus noise data vectors to minimize the sidelobe contributions from those components that do not match with the steering vector for a given search cell. Let R be the covariance matrix of the received signal and noise, and R=<XX$^+$> where <> denotes ensemble average over a

number of sequential data vectors X and "+" denotes Hermitian transpose. The minimum variance distortionless response (MVDR) method minimizes the variance at the output of a linear weighting of the hydrophone array subject to the distortionless constraint that signals in the steering direction have unity gain. The formulation minimizes the variance given by

$$S_{MVDR} = \mathrm{W}^{+}\mathrm{R}\ \mathrm{W}$$

with respect to the weighting W, subject to the unity gain constraint

$$\mathrm{W}^{+}\mathrm{A} = 1$$

where A is a steering vector. The MVDR weight vector W_{MVDR} can be derived as

$$\mathrm{W}_{MVDR} = \frac{\mathrm{R}^{-1}\mathrm{A}}{\mathrm{A}^{+}\mathrm{R}^{-1}\mathrm{A}}$$

where R^{-1} is matrix inversion. The MVDR output is

$$S_{MVDR} = \frac{1}{\mathrm{A}^{+}\mathrm{R}^{-1}\mathrm{A}}$$

Applying the eigen-value decomposition, the covariance matrix R can be decomposed into a set of eigenvectors V_i associated with a set of eigenvalues λ_i, so that

$$\mathrm{R} = \sum_{i=1}^{N} \lambda_i \mathrm{V}_i \mathrm{V}_i^{+}$$

and the inverse of the covariance matrix is given by

$$\mathrm{R}^{-1} = \sum_{i=1}^{N} \frac{1}{\lambda_i} \mathrm{V}_i \mathrm{V}_i^{+}$$

The MVDR weight vector becomes

$$\mathrm{W}_{MVDR} = \frac{\sum_{i=1}^{N} \frac{1}{\lambda_i}\left(\mathrm{V}_i^{+}\mathrm{A}\right)\mathrm{V}_i}{\sum_{i=1}^{N} \frac{1}{\lambda_i}\left|\mathrm{V}_i^{+}\mathrm{A}\right|^2}$$

The MVDR output becomes

$$S_{MVDR} = \left(\sum_{i=1}^{N} \frac{1}{\lambda_i}\left|\mathrm{V}_i^{+}\mathrm{A}\right|^2\right)^{-1}$$

An alternative way to obtain V_i and λ_i described in Section 1 is applying singular-value decomposition to a sample-matrix.

Without mismatch between data and model and when the signal is loud enough, the steering vector A is perfectly matched with signal eigenvector in the steering direction. The rest of eigenvectors are orthogonal to the steering vector and have no effect on the output. But, when mismatch is present, the steering vector is no longer orthogonal to the rest of eigenvectors. The noise vectors associated with the least significant eigenvalues then dominate the inverse processing and degrade the signal estimation.

All forms of mismatch are either deterministic or random. Deterministic mismatch degrades the signal estimation and causes bias in estimation, but it can be minimized if a prior knowledge is included in modeling the signal. Random mismatch degrades the signal estimation but will not bias the estimation. Random mismatch cannot be minimized so that robust algorithms were developed to tolerate it to a certain level. The white-noise-gain constrained (WNC) method referred to by Cox [3], dynamically adjusts the sensor noise level by adding white noise power to the diagonal elements of the covariance matrix subject to an inequality constraint on the sensor noise gain. Adding noise expands the noise space and effectively eliminates small eigenvalues that would otherwise dominate the sum in the MVDR output calculation due to mismatch.

The MVDR white noise processing gain, defined as the amplitude squared of the weight vector $\left|\mathrm{W}_{MVDR}\right|^2$, is directly proportional to the signal-to-noise ratio (SNR). The MVDR signal degradation due to mismatch is inversely proportional to the SNR. At low SNR, the white noise processing gain approaches unity (the conventional linear processing noise gain) and the mismatch effect is negligible. At high SNR, the white noise processing gain is high and the MVDR output is very sensitive to mismatch. For each steering direction, the WNC method dynamically adjusts the sensor noise level by adding white noise to the diagonal elements of the covariance matrix. Adding white noise lowers the "apparent" SNR so that the processing becomes less sensitive to mismatch. Adding white noise, in the amount ε, to the diagonal elements of the covariance matrix is the same as adding ε to each eigenvalues without modifying the eigenvectors. The WNC weight vector W_{WNC} that result is

$$\mathrm{W}_{WNC} = \frac{\sum_{i=1}^{N} \frac{1}{\lambda_i + \varepsilon}\left(\mathrm{V}_i^{+}\mathrm{A}\right)\mathrm{V}_n}{\sum_{i=1}^{N} \frac{1}{\lambda_i + \varepsilon}\left|\mathrm{V}_i^{+}\mathrm{A}\right|^2}$$

and the WNC output is

$$S_{WNC} = \frac{\sum_{i=1}^{N} \frac{\lambda_i}{\left(\lambda_i + \varepsilon\right)^2}\left|\mathrm{V}_i^{+}\mathrm{A}\right|^2}{\left(\sum_{i=1}^{N} \frac{1}{\lambda_i + \varepsilon}\left|\mathrm{V}_i^{+}\mathrm{A}\right|^2\right)^2}$$

There are many approaches to determine the amount of white noise to add in the WNC processing. In this study the following algorithm is used. For each steering direction, the MVDR white noise processing gain and the MVDR output are calculated. If the white noise processing gain falls below a pre-selected constraining

value, the MVDR processing is used. If the white noise processing gain is above the constraining value, an amount of white noise that equals the MVDR output is added in the WNC processing.

In this paper all adaptive beamforming (ABF) refer to WNC adaptive beamforming with a 3-dB constraint. The phone-space adaptive beamforming (PS_ABF) refers to the WNC adaptive beamforming performing on the hydrophone sample-matrix with a calculated phone steering vector.

4. Subarray Beam-space Adaptive Beamforming (SABS_ABF)

Subarray beam-space adaptive beamforming is a two-stage processing. It has been studied [4] with emphasis on its advantage of rank reduction for fast adaptation. In this study, our emphasis is on using the updated AEL to compensate the temporal variation of a received signal due to rapid changes in array shape. Figure 4 shows the

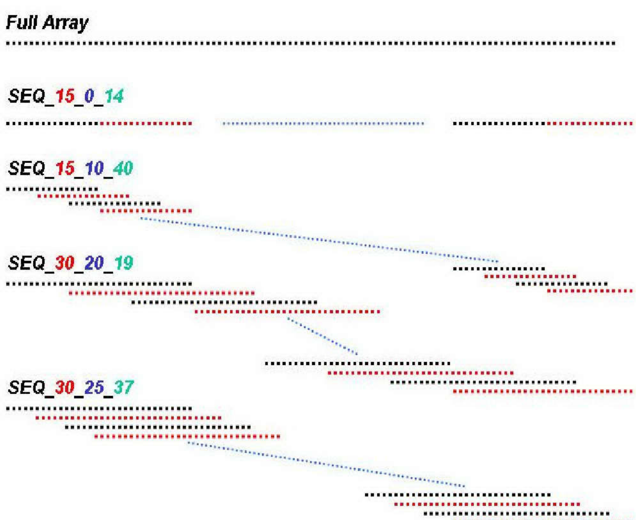

Figure 4: Subarray configurations used in this study

full-array and four Subarray configurations that are considered in this study. The notations in each configuration are SEQuential, number of hydrophones in each subarray, subarray overlap, and number of subarrays. For example, SEQ_15_10_40 is a configuration of 15-phone subarrays in a sequential format with overlap of 10 phones and a total of 40 subarrays.

Let $\{1,2,\ldots,S\}$ be a set of hydrophones in one of the subarrays, the range-focus steering vector of the mth subarray at search cell r is calculated as

$$\mathrm{A}_m^+(\mathrm{r},t) = \frac{1}{\sqrt{S}}\begin{bmatrix} e^{-i\varphi_{m,1}(t)} & e^{-i\varphi_{m,2}(t)} & \cdots & e^{-i\varphi_{m,S}(t)} \end{bmatrix}$$

where

$$\varphi_{m,s}(t) = 2\pi f\left|\mathrm{r} - \mathrm{r}_{m.s}(t)\right|/c$$

c is the sound speed and $\mathrm{r}_{m,s}(t)$ is the measured position of the sth hydrophone in the mth subarray at time t. In the first stage SABS_ABF performs subarray conventional beamforming using the updated subarray steering vectors and transforms the phone-space sample-matrix into a beam-space sample-matrix

$$(\mathrm{r},t) = \begin{bmatrix} b_1(\mathrm{r},t) & b_1(\mathrm{r},t+\Delta t) & \ldots & b_1(\mathrm{r},t+(K-1)\Delta t) \\ b_2(\mathrm{r},t) & b_2(\mathrm{r},t+\Delta t) & \ldots & b_2(\mathrm{r},t+(K-1)\Delta t) \\ \vdots & \vdots & \vdots & \vdots \\ b_M(\mathrm{r},t) & b_M(\mathrm{r},t+\Delta t) & \ldots & b_M(\mathrm{r},t+(K-1)\Delta t) \end{bmatrix}$$

where

$$b_m(\mathrm{r},t) = \quad {}^{+}(\mathrm{r},t) \bullet \quad (t)$$

is the conventional beamformer response of the m^{th} subarray and $X_m(t)$ is the data vector of the m^{th} subarray at time t. In the first stage SABS_ABF also transforms the phone-space steering vector into a beam-space steering vector. Let

$$\tilde{\mathrm{A}}_b^+(\mathrm{r},t) = \begin{bmatrix} \tilde{A}_{b,1}^*(\mathrm{r},t) & \tilde{A}_{b,2}^*(\mathrm{r},t) & \cdots & \tilde{A}_{b,M}^*(\mathrm{r},t) \end{bmatrix}$$

where

$$\tilde{A}_{b,m} = \mathrm{A}_m^+(\mathrm{r},t) \bullet \mathrm{A}_m(\mathrm{r},t)$$

the beam-space steering vector is calculated as

$$\mathrm{A}_b(\mathrm{r},t) = \tilde{\mathrm{A}}_b(\mathrm{r},t) / \left|\tilde{\mathrm{A}}_b(\mathrm{r},t)\right|$$

For a constant amplitude non-fading signal, the beam-space steering vector is simply a unity vector with a uniform weight of $1/\sqrt{M}$ on each subarray. In the second stage SABS_ABF performs white-noise-constrained adaptive beamforming described in Section 3 with the calculated beam-space sample-matrix and the beam-space steering vector.

5. Simulation Results

The simulation geometry has been described in Section 1 and a 0-dB white noise is injected in all simulations. For target-only, Figure 5 shows the WNC ABF responses along the target track. Assuming array is straight (No AEL), PS_ABF experiences significant mismatch loss during turn. When the measured mean AEL is used, the mismatch loss in PS_ABF is reduced, but there still is more than 5 dB signal spread loss in the turn due to rapid changes in array shape within the 30-s processing interval. SABF_ABF shows success in holding the target through the turn. For target-only, Figures 6 and 7show the bearing-time responses (BTRs) resulted from PS_ABF and SABS_ABF for a 0-dB target. The results show that SABS_ABF not only reduces the signal spread loss but also reduces the angular spread of the target during the turn.

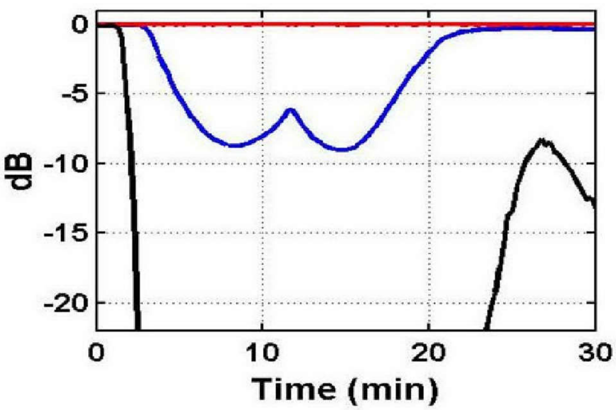

Figure 5: WNC ABF responses along target track, black curve is result of PS_ABF without AEL, blue curve is result of PS_ABF with mean AEL, and red curve is result of SABS_ABF for SEQ_15_10_41 configuration.

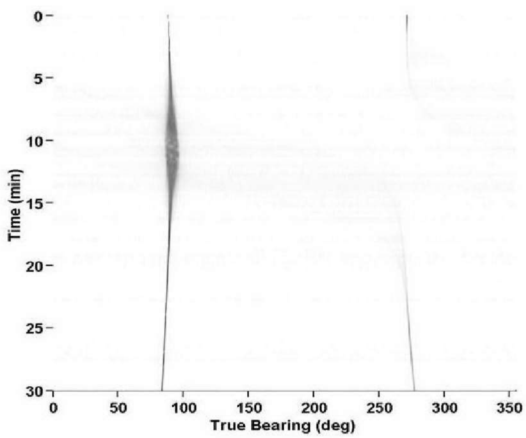

Figure 6: BTR of PS_ABF for a 0-dB target

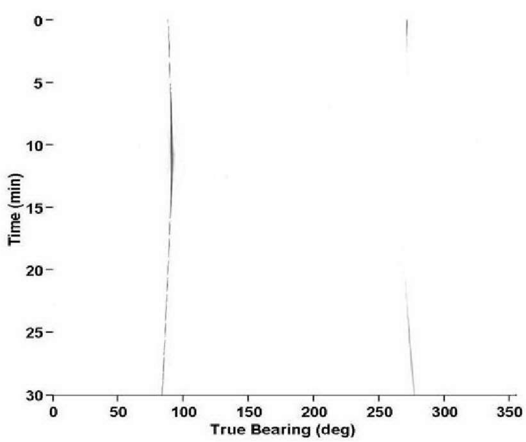

Figure 7: BTR of SABS_ABF with SEQ_15_10_41 configuration for a 0-dB target

Figures 8 and 9 show the WNC ABF results for a weak target in a stressful environment. In this case, the target power is set at -18 dB, the own-ship and the other two interferers are set at 15 dB. The PS_ABF result shows that target is lost in the interference in turn. The SABS_ABF result shows a continuous target-holding through turn under such stressful condition.

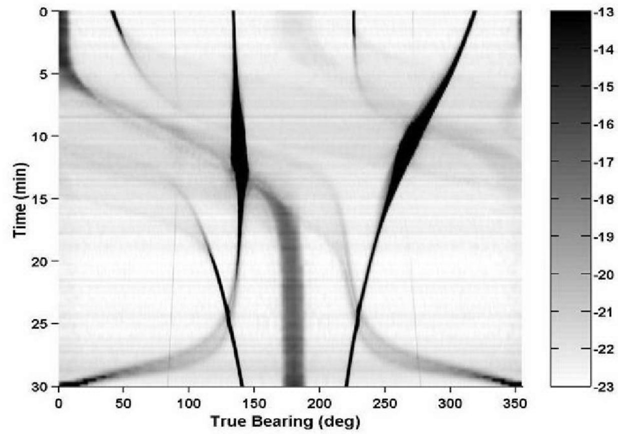

Figure 8: BTR of PS_ABF for a weak target in a stressful environment

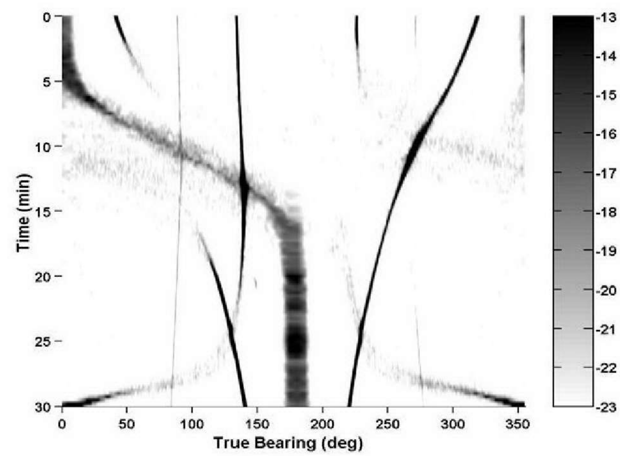

Figure 9: BTR of SABS_ABF with SEQ_15_10_41 configuration for a weak target in a stressful environment

Figures 7 and 9 are results of SABS_ABF with SEQ_15_10_40 subarray configuration where two consecutive subarrays have a 66% overlap and the centers are shifted by a distance of 5-phone spacing. Figure 10 shows result of SABS_ABF with SEQ_15_0_14 configuration where two consecutive subarrays have no overlap and the centers are shifted by a distance of 15-phone spacing. It shows that overlapping the subarrays provides better suppression of signal sidelobes. Figure 11

shows result of SABS_ABF with SEQ_30_10_37 configuration where two consecutive subarrays have a 66% overlap and the centers are shifted by a distance of 10-phone spacing. Signal sidelobes are still noticeable in this case. Figure 12 shows result of SABS_ABF with SEQ_30_5_37 configuration where two consecutive subarrays have a 83% overlap and the centers are shifted by a distance of 5-phone spacing. Signal sidelobes are well behaved as seen in SEQ_15_5_40. This says that the distance between the centers of two consecutive subarrays is an important parameter for SABS_ABF processing.

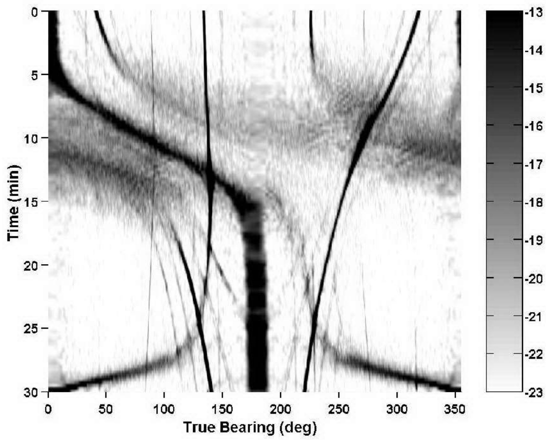

Figure 10: BTR of SABS_ABF with SEQ_15_0_14 configuration for a weak target in a stressful environment

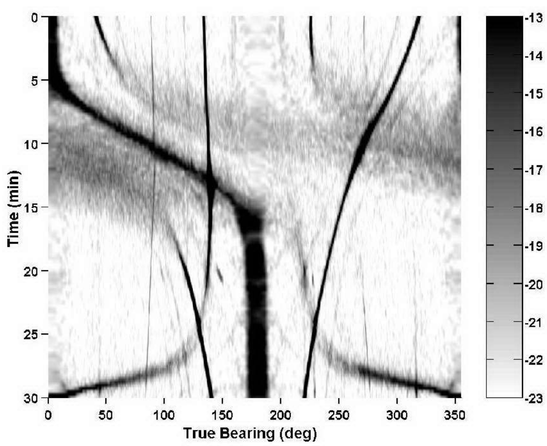

Figure 11: BTR of SABS_ABF with SEQ_30_10_19 configuration for a weak target in a stressful environment

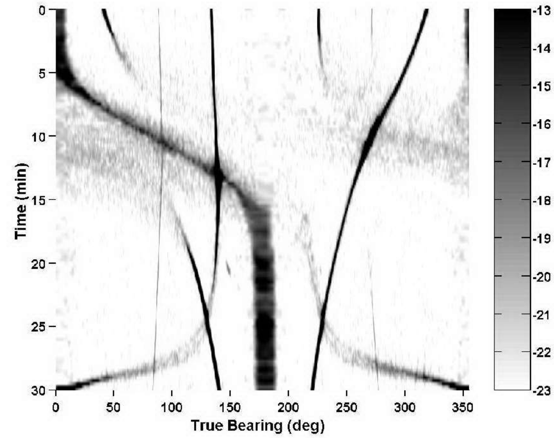

Figure 12: BTR of SABS_ABF with SEQ_30_5_37 configuration for a weak target in a stressful environment

6. Summary

In this paper we address the issue of signal spread loss in a phone-space sample-matrix due to rapid changes of array shape within a processing interval when array is in maneuvering. The loss significantly affects detection and tracking of a weak target. SBAS_ABF uses the updated AEL to compensate the temporal variation of the received signal so that signal in the beam-space sample-matrix becomes stationary during array maneuvering. It is shown that SABS_ABF not only has the advantage of reducing rank for fast adaptation, but also improves target detection and tacking through severe array maneuvering.

Reference:

[1]“Beamspace Adaptive beamforming for Hydrodynamic Towed Array Self-Noise Cancellation” V. E. Premus, S. M. Kogon, and J. Ward, ASAP 2001

[2]“Model Based Array Element Localization for Single and Multiline Towed Arrays”, J. P. Ianniello, R. B. Evans, and B. Sperry, ASAP 2003

[3]“Robust Adaptive Beamforming,” H. Cox, IEEE Trans. On Acoustics, Speech m and Signal Processing, vol. ASSP 35, pp. 1365-1376, Oct. 1987.

[4]“Sub-Aperture Beamspace Adaptive Processing,” H. Freese, B. Sperry, and K. Votow, ASAP 2003.

Subarray Beam-Space Adaptive Beamforming for A Dynamic Long Towed-Array

Dr. Yung P. Lee, SAIC/McLean

Herb Freese, SAIC/McLean

William W. Lee, Univ. of Maryland

17 March, 2004

Presented at ASAP 2004, MIT Lincoln Lab

OUTLINE

- ***Background & Issues***
- ***White-Noise-Constrained Adaptive Beamforming (WNC_ABF)***
- ***Subarray Beam-Space Adaptive Beamforming (SABS_ABF)***
- ***Simulation Results***
- ***Summary***

Issues of Long Towed-Array Through A Dynamic Maneuver

- ***Flow Noise***
  - *"Beamspace Adaptive beamforming for Hydrodynamic Towed Array Self-Noise Cancellation" V. E. Premus, S. M. Kogon, and J. Ward, ASAP 2001*
- ***Change in Array Shape – Array Element Location (AEL)***
  - *"Model Based Array Element Localization for Single and Multiline Towed Arrays", J. P. Ianniello, R. B. Evans, and B. Sperry, ASAP 2003*
- ***Signal Spread in Phone-Space Sample-Matrix***
  - ***Signal Structure Changes Within Processing Interval Due to Array Motion***
    - ***Signal Coherence Loss among Hydrophones***
    - ***Spread in Singular-Value/Singular Vector or Eigenvalue/Eigenvector***

Simulation Geometry – 180° Turn

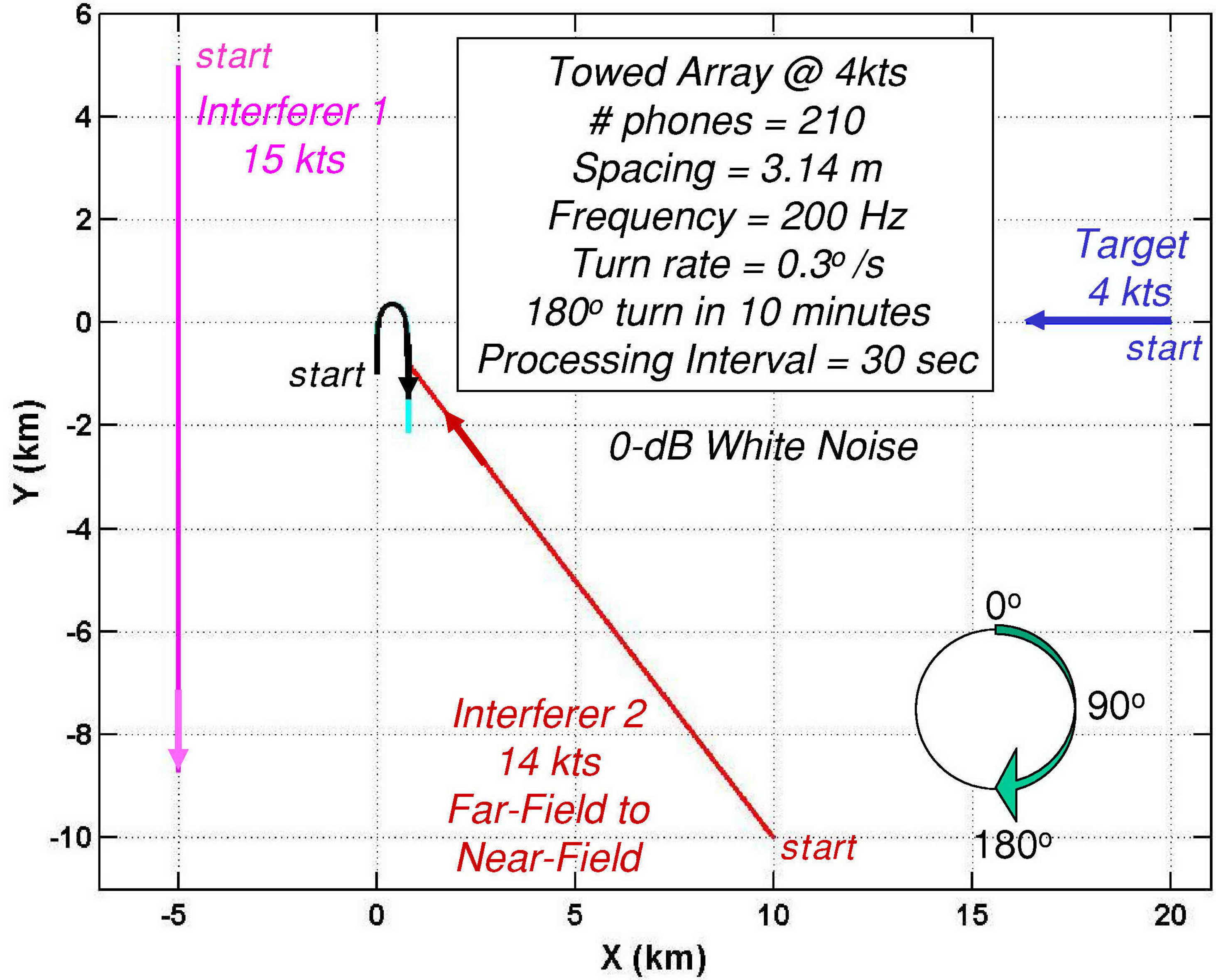

Signal Coherence Loss Through Turn

Target Only, Processing Interval = 30 sec

Signal Coherence relative to phone 1

$$SC_n(t) = \frac{\left|\sum_{k=0}^{N-1} x_1^*(t+k\Delta t) \bullet x_n(t+k\Delta t)\right|^2}{\sum_{k=0}^{N-1}\left|x_1(t+k\Delta t)\right|^2 \bullet \sum_{n=0}^{N-1}\left|x_n(t+k\Delta t)\right|^2}$$

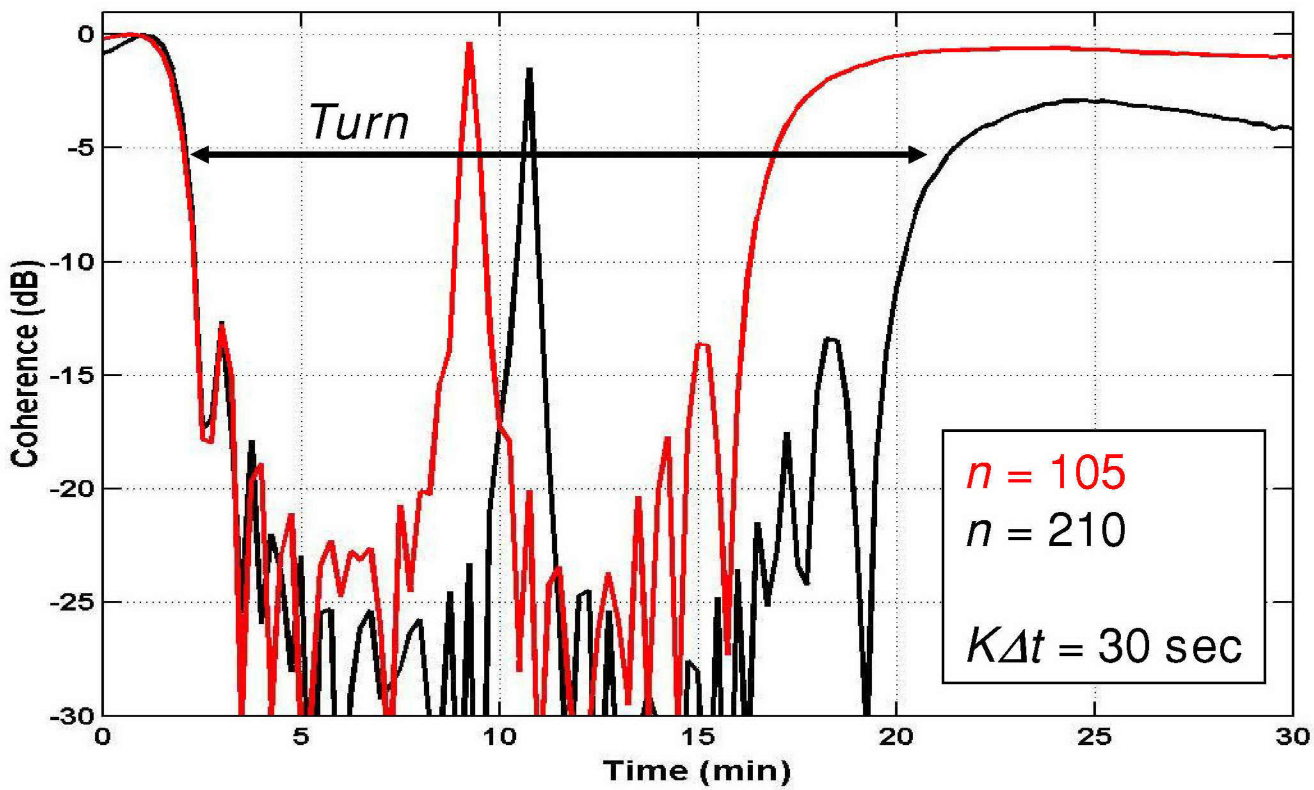

Phone-Space Singular-Value Spread Through Turn

Target Only, Processing Interval = 30 sec

Phone-Space Sample-Matrix

$$= \begin{bmatrix} x_1(t) & x_1(t+\Delta t) & x_1(t+2\Delta t) & \dots & x_1(t+(K-1)\Delta t) \\ x_2(t) & x_2(t+\Delta t) & x_2(t+2\Delta t) & \dots & x_2(t+(K-1)\Delta t) \\ \vdots & \vdots & \vdots & \vdots & \vdots \\ x_N(t) & x_N(t+\Delta t) & x_N(t+2\Delta t) & \dots & x_N(t+(K-1)\Delta t) \end{bmatrix}$$

Singular Value Decomposition (SVD)

$$X = V^{+} \Lambda \; U$$

$$\Lambda = \begin{bmatrix} \sqrt{\lambda_1} & 0 & \cdots & 0 \\ 0 & \sqrt{\lambda_2} & \cdots & 0 \\ \vdots & \vdots & \ddots & \vdots \\ 0 & 0 & \cdots & \sqrt{\lambda_N} \end{bmatrix}$$

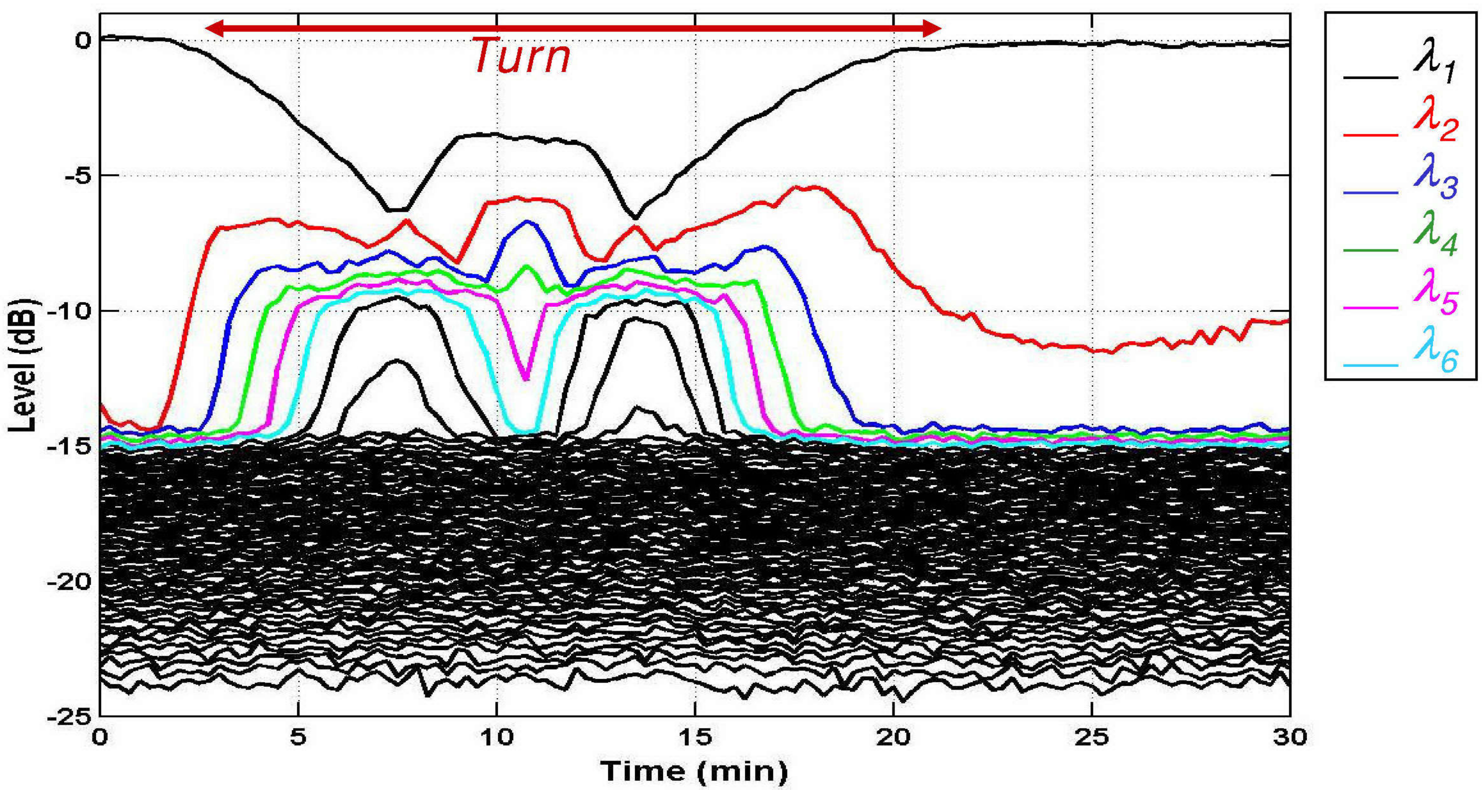

OUTLINE

- Background & Issues
- White-Noise-Constrained Adaptive Beamforming (WNC_ABF)
- Subarray Beam-Space Adaptive Beamforming (SABS_ABF)
- Simulation Results
- Summary

White-Noise-Constrained Adaptive Beamforming (WNC_ABF)

** All ABFs refer to WNC_ABF with δ=3 dB

** PS_ABF refers to WNC_ABF performing on the phone-space covariance or sample matrix with the calculated phone-space steering vectors

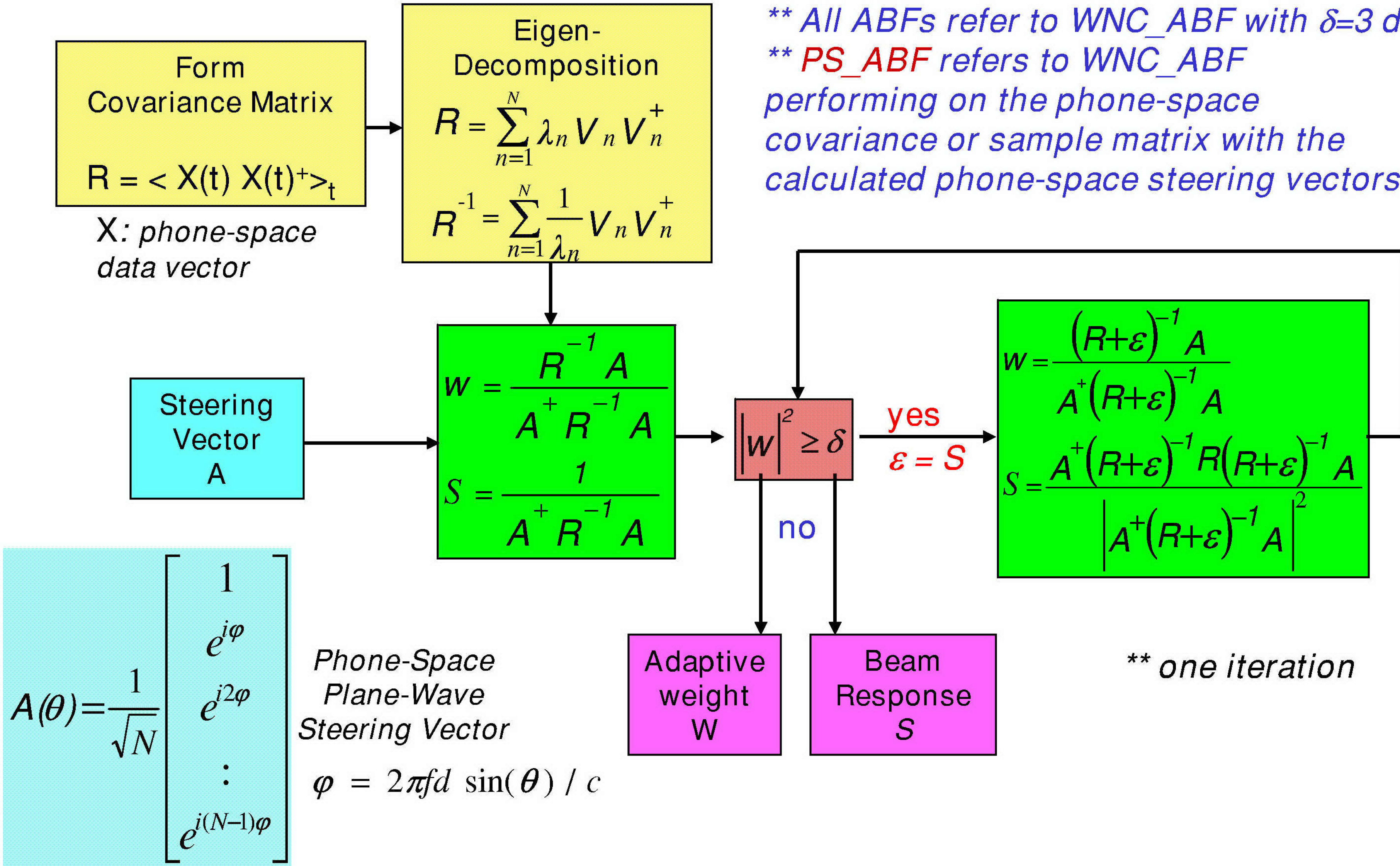

WNC_ABF - Alternatives

Phone-Space Sample-Matrix

$$= \begin{bmatrix} x_1(t) & x_1(t+\Delta t) & x_1(t+2\Delta t) & \dots & x_1(t+(K-1)\Delta t) \\ x_2(t) & x_2(t+\Delta t) & x_2(t+2\Delta t) & \dots & x_2(t+(K-1)\Delta t) \\ \vdots & \vdots & \vdots & \vdots & \vdots \\ x_N(t) & x_N(t+\Delta t) & x_N(t+2\Delta t) & \dots & x_N(t+(K-1)\Delta t) \end{bmatrix}$$

Phone-Space Range-Focus Steering Vector

$$\varphi_n = 2\pi f \mid \mathrm{r} - \mathrm{r}_n \mid / c$$

$$A(\mathrm{r}) = \frac{1}{\sqrt{N}} \begin{bmatrix} e^{i\varphi_1} \\ e^{i\varphi_2} \\ \vdots \\ e^{i\varphi_N} \end{bmatrix}$$

Sample-Matrix
X

Singular Value Decomposition (SVD)

$$X = \mathrm{V}^{+} \mathbf{\Lambda} \ \mathrm{U}$$

$$\mathbf{\Lambda} = \begin{bmatrix} \sqrt{\lambda_1} & 0 & \cdots & 0 \\ 0 & \sqrt{\lambda_2} & \cdots & 0 \\ \vdots & \vdots & \ddots & \vdots \\ 0 & 0 & \cdots & \sqrt{\lambda_N} \end{bmatrix} \qquad V = \begin{bmatrix} V_1 & V_2 & \cdots & V_N \end{bmatrix}$$

$$R^{-1} = \sum_{n=1}^{N} \frac{1}{\lambda_n} V_n V_n^{+}$$

Steering Vector
A

$$w = \frac{R^{-1} A}{A^{+} R^{-1} A}$$

$$S = \frac{1}{A^{+} R^{-1} A}$$

$$|w|^2 \geq \delta$$

yes

$\varepsilon = S$

$$w = \frac{(R+\varepsilon)^{-1} A}{A^{+}(R+\varepsilon)^{-1} A}$$

$$S = \frac{A^{+}(R+\varepsilon)^{-1} R (R+\varepsilon)^{-1} A}{\left| A^{+}(R+\varepsilon)^{-1} A \right|^2}$$

no

Adaptive weight
W

Beam Response
S

OUTLINE

- ***Background & Issues***
- ***White-Noise-Constrained Adaptive Beamforming (WNC_ABF)***
- ***Subarray Beam-Space Adaptive Beamforming (SABS_ABF)***
  - *"Sub-Aperture Beamspace Adaptive Processing" H. Freese, B. Sperry, and K. Votaw, ASAP 2003*
    - *emphasized on reduced rank and fast adaptation*
  - *This study emphasizes on using updated AEL to compensate signal structure changes from snapshot to snapshot due to rapid changes in array shape so that signal in the beam-space becomes "stationary"*
    - *Coherence across subarrays*
    - *Less spread in singular-value or eigen-decomposition*
- ***Simulation Results***
- ***Summary***

The 1st Stage of SABS_ABF

Subarray CBF with Updated AEL

$$\varphi_n(t) = 2\pi f \left| \mathrm{r} - \boxed{\mathrm{r}_n(t)} \right| / c$$

$\mathrm{r}_n(t)$ *is the updated AEL*

$$\tilde{A}(\mathrm{r},t) = \begin{bmatrix} e^{i\varphi_1(t)} & e^{i\varphi_1(t+\Delta t)} & \cdots & e^{i\varphi_1(t+(K-1)\Delta t)} \\ e^{i\varphi_2(t)} & e^{i\varphi_2(t+\Delta t)} & \cdots & e^{i\varphi_2(t+(K-1)\Delta t)} \\ \vdots & \vdots & \vdots & \vdots \\ e^{i\varphi_N(t)} & e^{i\varphi_N(t+\Delta t)} & \cdots & e^{i\varphi_N(t+(K-1)\Delta t)} \end{bmatrix}$$

Phone-Space Sample-Matrix

$$(t) = \begin{bmatrix} x_1(t) & x_1(t+\Delta t) & \ldots & x_1(t+(K-1)\Delta t) \\ x_2(t) & x_2(t+\Delta t) & \ldots & x_2(t+(K-1)\Delta t) \\ \vdots & \vdots & \vdots & \vdots \\ x_N(t) & x_N(t+\Delta t) & \ldots & x_N(t+(K-1)\Delta t) \end{bmatrix}$$

Subarray Steering Vector

$$_m(\mathrm{r},t) = \tilde{\ }_{m,\{s\}}(\mathrm{r},t) \Big/ \sqrt{S}$$

Subarray Data Vector

$$_m(t) = \ _{m,\{s\}}(t)$$

$$\tilde{A}_b(\mathrm{r},t) = \begin{bmatrix} \tilde{A}_{b,1}(t) & \tilde{A}_{b,1}(t+\Delta t) & \cdots & \tilde{A}_{b,1}(t+(K-1)\Delta t) \\ \tilde{A}_{b,2}(t) & \tilde{A}_{b,2}(t+\Delta t) & \cdots & \tilde{A}_{b,2}(t+(K-1)\Delta t) \\ \vdots & \vdots & \vdots & \vdots \\ \tilde{A}_{b,M}(t) & \tilde{A}_{b,M}(t+\Delta t) & \cdots & \tilde{A}_{b,M}(t+(K-1)\Delta t) \end{bmatrix}$$

$$(\mathrm{r},t) = \begin{bmatrix} b_1(t) & b_1(t+\Delta t) & \ldots & b_1(t+(K-1)\Delta t) \\ b_2(t) & b_2(t+\Delta t) & \ldots & b_2(t+(K-1)\Delta t) \\ \vdots & \vdots & \vdots & \vdots \\ b_M(t) & b_M(t+\Delta t) & \ldots & b_M(t+(K-1)\Delta t) \end{bmatrix}$$

Beam-Space Sample-Matrix

Beam-Space Steering Vector

$$\tilde{A}_{b,m}(t) = \ _m^{+}(\mathrm{r},t) \bullet \ _m(\mathrm{r},t)$$

$$\mathrm{A}_b(\mathrm{r},t) = \tilde{\mathrm{A}}_b(\mathrm{r},t) \Big/ \sqrt{M}$$

Subarray CBF Response

$$b_m(t) = \ _m^{+}(\mathrm{r},t) \bullet \ _m(t)$$

The 2nd Stage of SABS_ABF

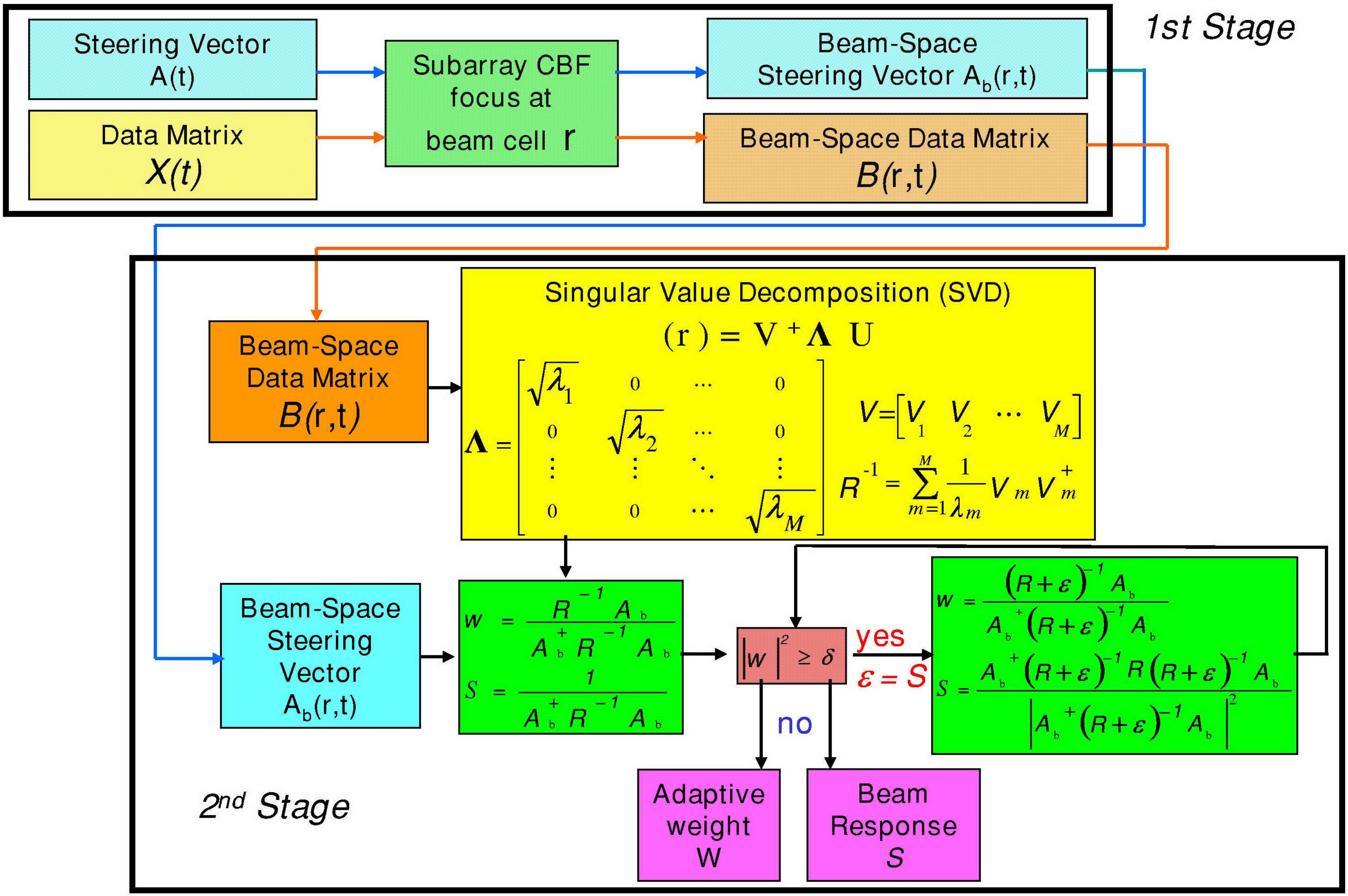

SubArray Selection

Sequential_ # phones in subarray _overlap_ # subarrays

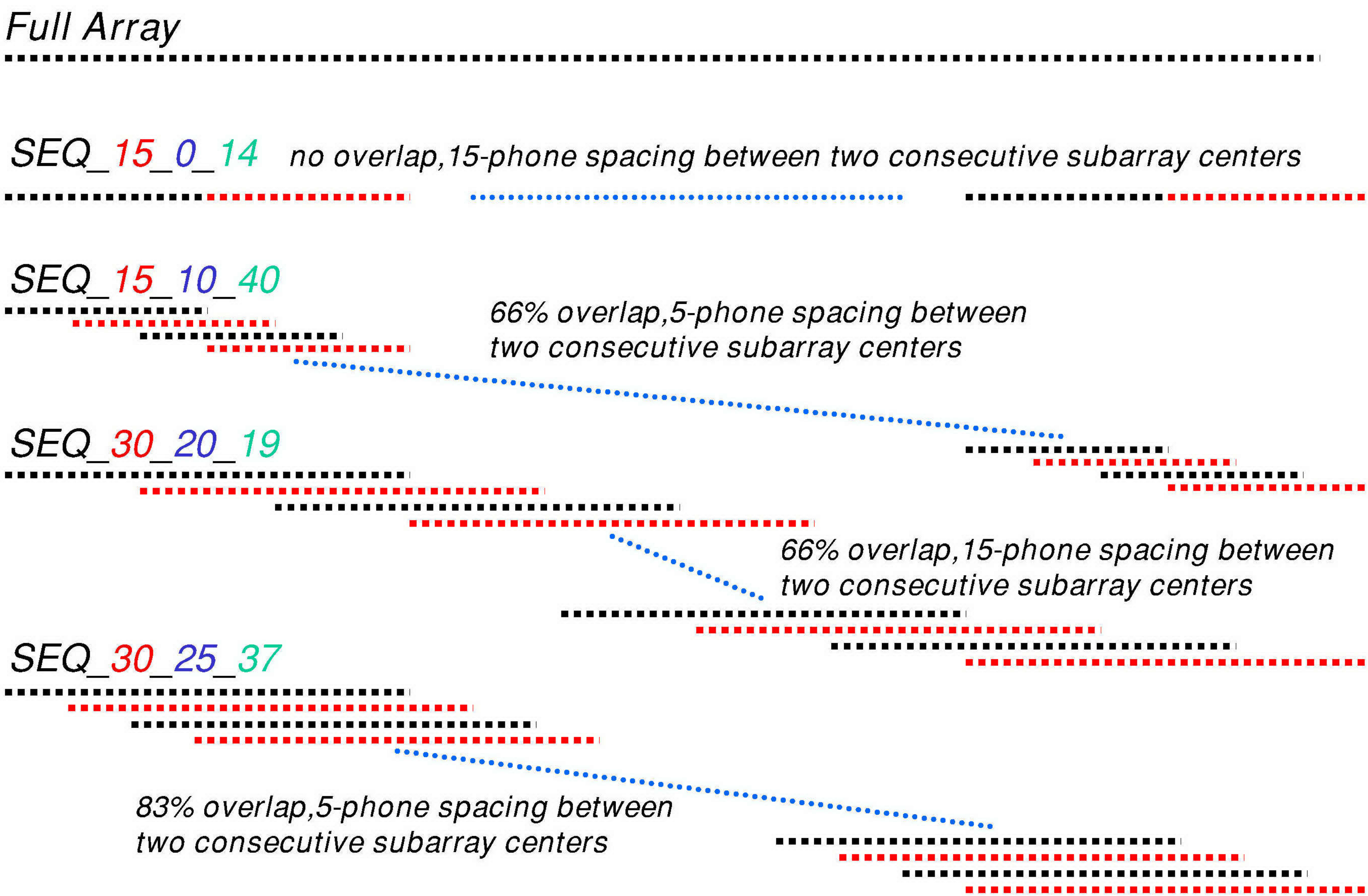

OUTLINE

- Background & Issues
- White-Noise-Constrained Adaptive Beamforming (WNC_ABF)
- Subarray Beam-Space Adaptive Beamforming (SABS_ABF)
- Simulation Results
- Summary

Beam-Time Responses Along Target Track

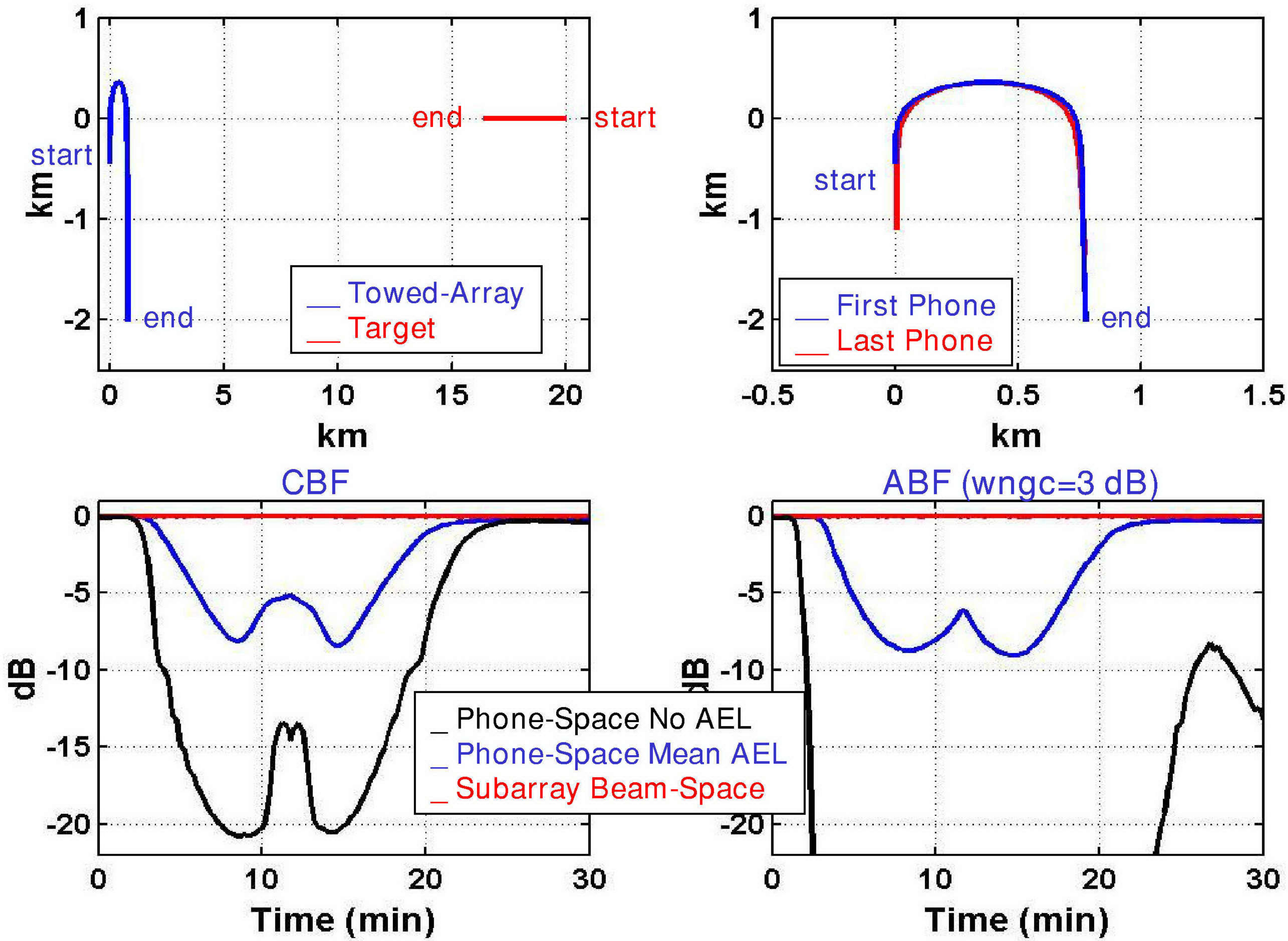

Bearing-Time Responses

Target Only (0 dB)

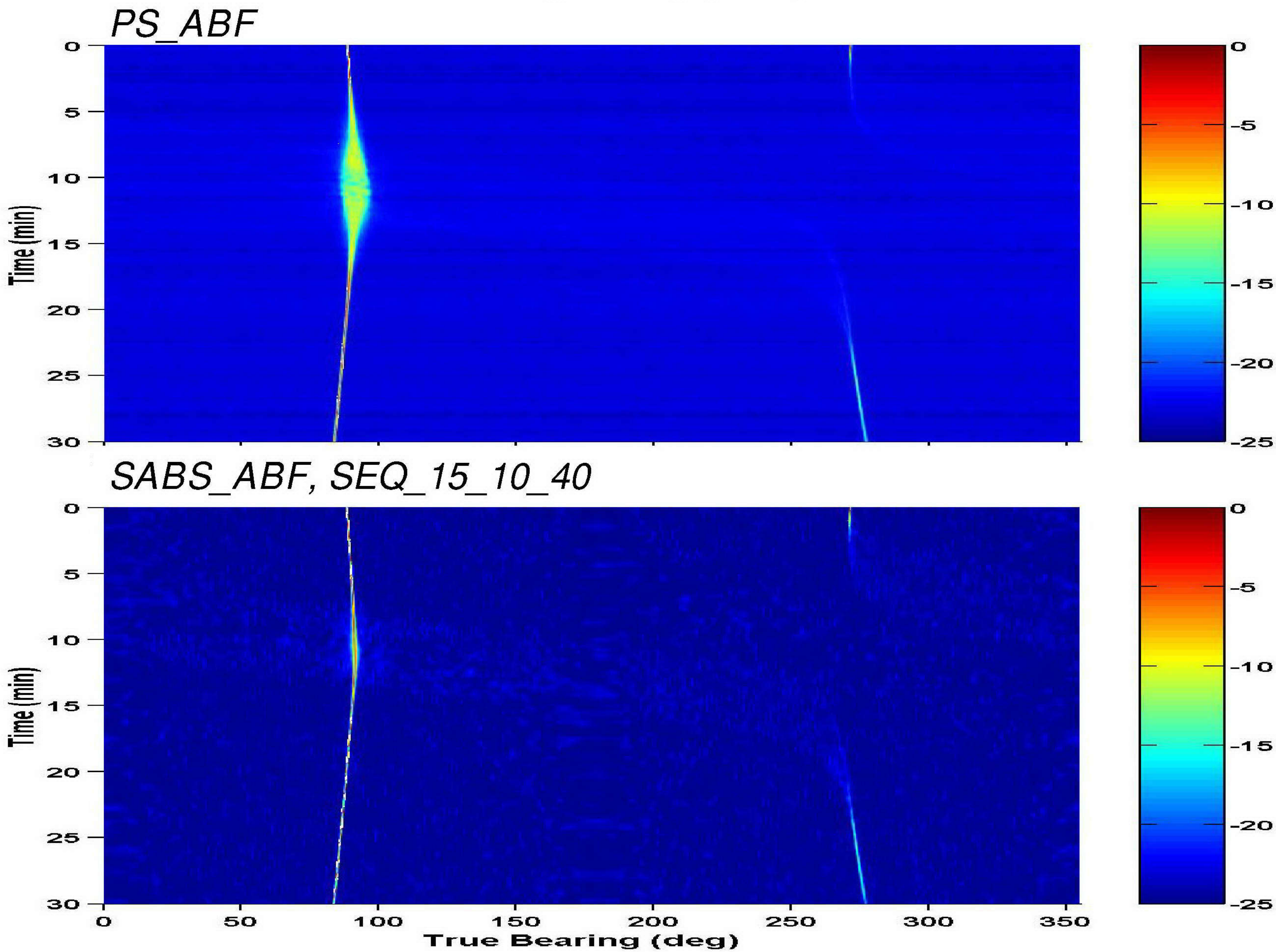

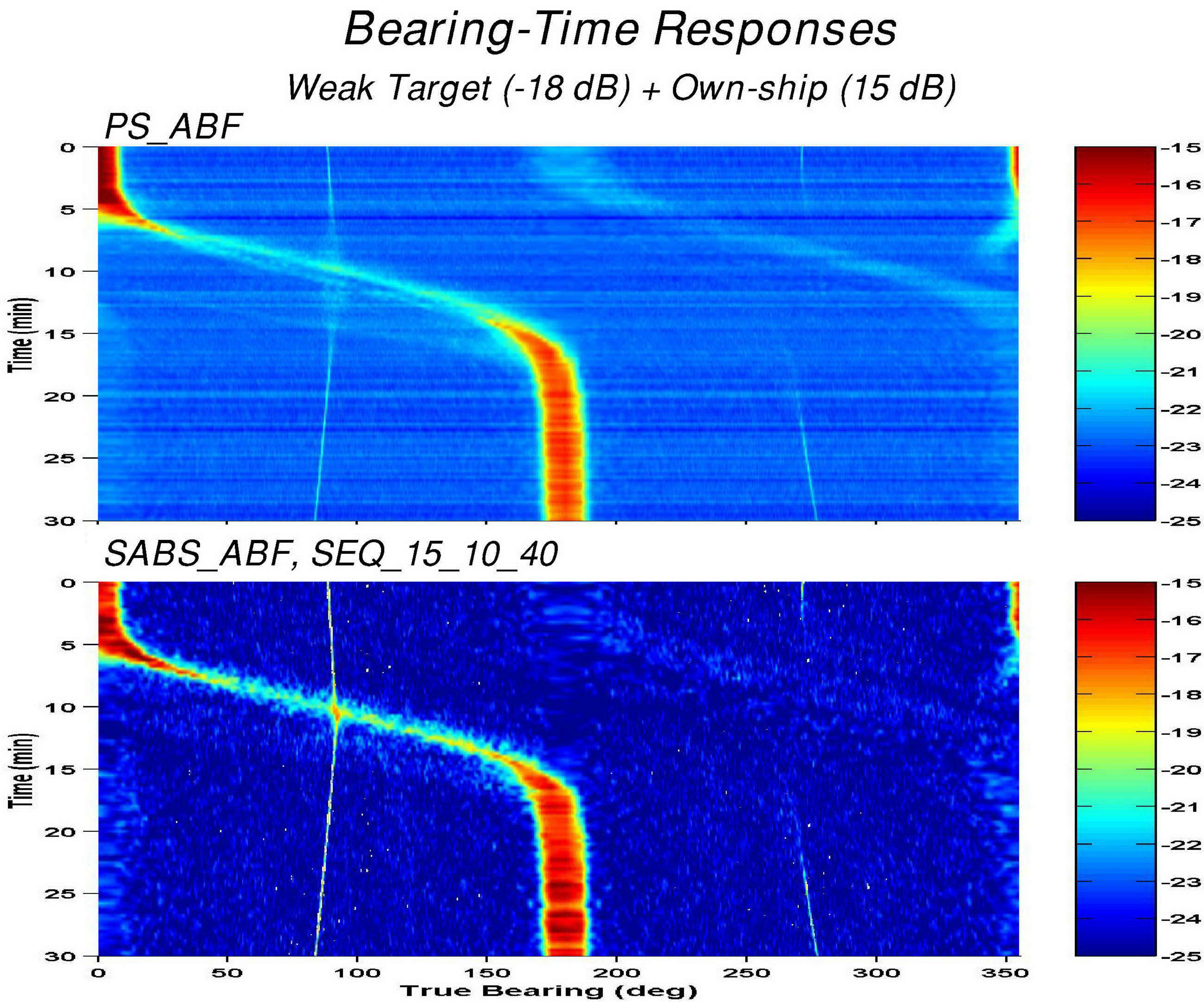
Bearing-Time Responses
Weak Target (-18 dB) + Own-ship (15 dB)
PS_ABF
SABS_ABF, SEQ_15_10_40
Time (min)
True Bearing (deg)
0
5
10
15
20
25
30
50
100
150
200
250
300
350
-15
-16
-17
-18
-19
-20
-21
-22
-23
-24
-25

Bearing-Time Responses

Weak Target (-18 dB) + Own-ship (15 dB) + Interferers (15 dB)

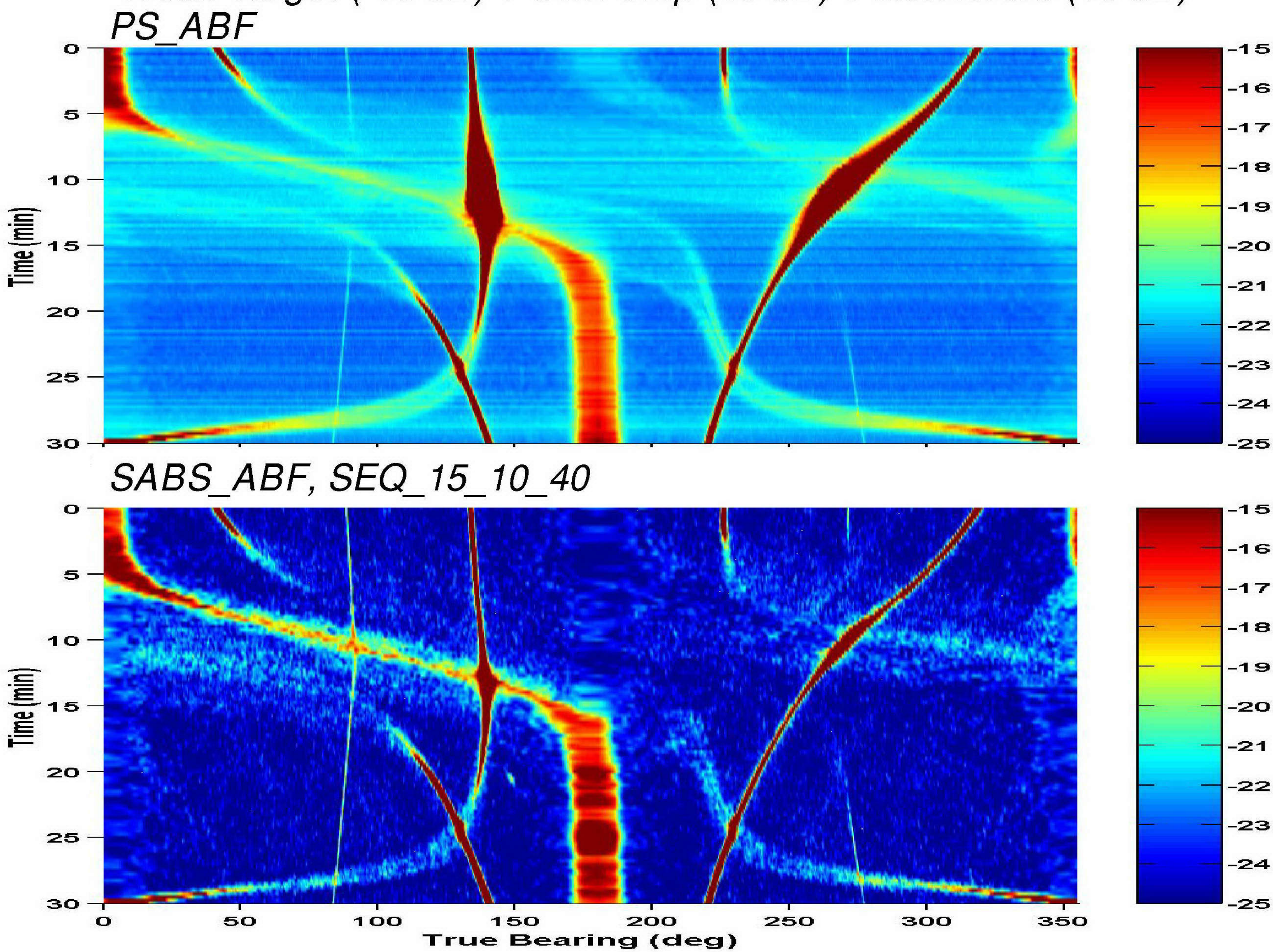

SABS_ABF Bearing-Time Responses

Weak Target (-18 dB) + Own-ship (15 dB) + Interferers (15 dB)

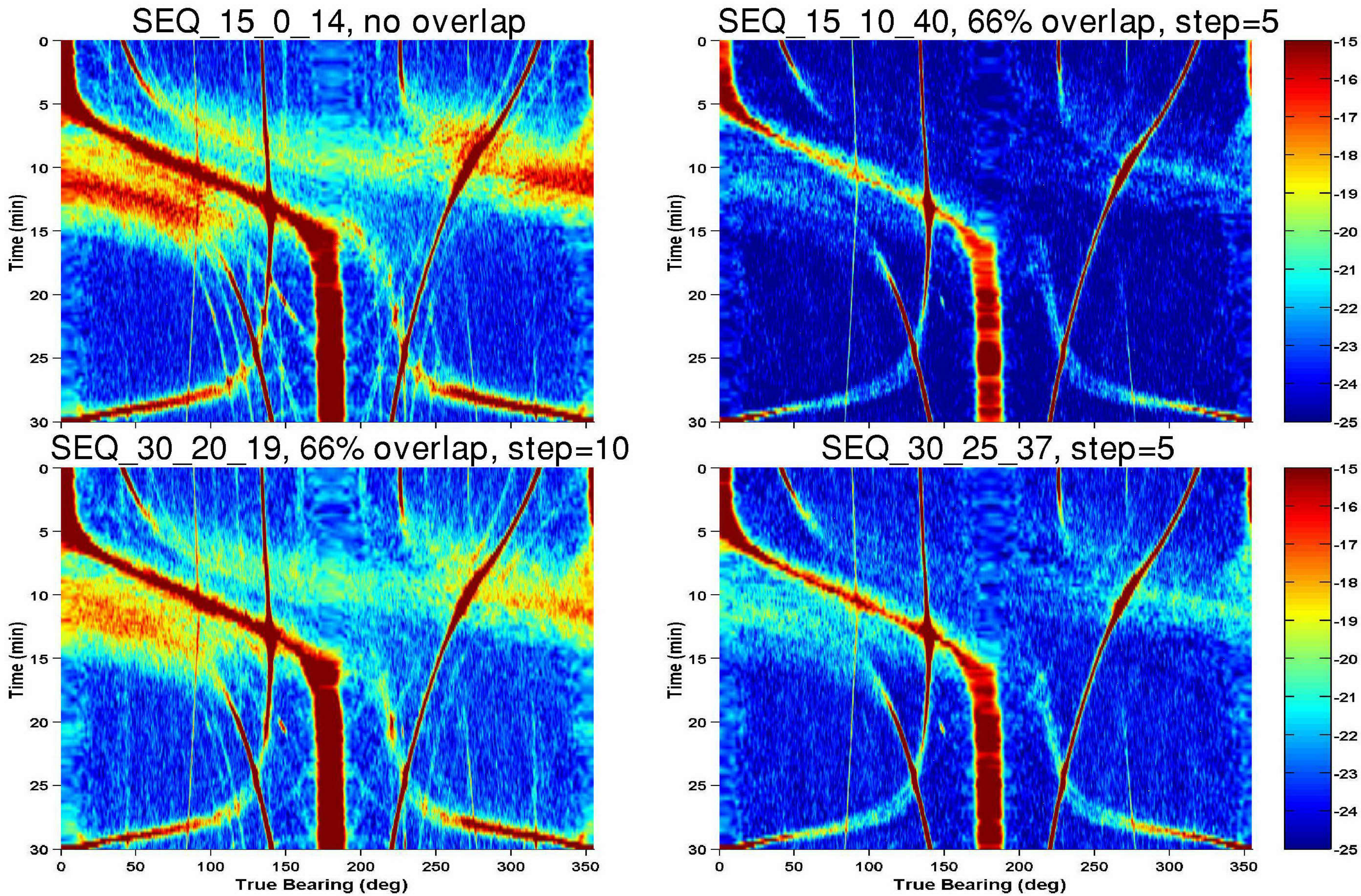

SUMMARY

- ***Subarray Beam-Space ABF with updated AEL compensation recovers signal spreading loss and provides continuous target holding through array maneuvering.***

- ***Beam-space ABF involves extensive computation***
  - ***Try Fast ABF such as Multi-Stage Wiener Filter***

- ***What's the rule-of-thumb for subarray selection?***
  - ***Distance between two consecutive subarray centers is an important parameter.***

- ***Is there significant benefit for ABF-ABF vs CBF-ABF?***